ELSEVIER

Journal of Hazardous Materials 46 (1996) 93–104

JOURNAL OF HAZARDOUS MATERIALS

Modelling boiling delay and transient level swell during emergency pressure relief of liquefied gases

B. Boesmans*, J. Berghmans

K.U. Leuven, Department of Mechanical Engineering, Celestijnenlaan 300 A, B-3001 Leuven-Heverlee, Belgium

Received 1 May 1994; accepted 5 December 1994

Abstract

A one-dimensional non-equilibrium model is presented for transient level swell during emergency pressure relief of liquefied gases. The model results are compared to small-scale pressure relief experiments. The effects of thermal non-equilibrium on level swell are summarized and it is shown that non-equilibrium effects are particularly important in small-scale vessels.

Keywords: Pressure relief; Safety valves; Boiling delay; Level swell

1. Introduction

This study deals with the boil-up phenomenon which occurs during emergency pressure relief of liquefied gases, stored at a pressure above ambient. This subject is of vital importance in chemical process safety [1]. Vessels containing liquefied gases have to be protected against overpressures, resulting from unwanted heating of the vessel contents (e.g. due to a surrounding fire or due to a runaway chemical reaction). Very often emergency pressure relief for such vessels is provided by a safety valve or a bursting disc installed at the top of the vessel. During the sudden depressurization immediately following the activation of the pressure relief system, part of the vessel contents flashes, which may cause the liquid level to rise to the top of the vessel and result in two-phase flow through the relief system.

It is well established that relief performance is severely affected by the flow conditions in the relief system. Two-phase flow in particular is known to cause *worse* pressure relief than single phase flow through the same relief system. The flow conditions in the relief system are determined by the level swell behaviour of the vessel contents, which should therefore be taken into account for an adequate design of the relief system.

* Corresponding author.

SSDI 0304-3894(95)00061-5

In most of the currently available pressure relief models, such as the well known SAFIRE model [2], an integral description of level swell is used (based on an assumption about the vapour generation distribution in the vessel), and thermal equilibrium is assumed. These models are aimed at predicting *quasi-steady* level swell behaviour and are not valid during the initial level swell transient, which occurs immediately after the activation of the pressure relief system. Transient level swell is affected by non-equilibrium flashing vapour generation (including boiling delay, nucleation and bubble growth) and by the dynamics of void propagation in the two-phase mixture. Therefore a one-dimensional non-equilibrium model is needed to describe transient level swell adequately. In this paper such a model is presented and compared to the results of small-scale pressure relief experiments.

2. Equilibrium model

Pressure relief models of various degrees of complexity are currently available. Many of these are essentially very similar to the SAFIRE model resulting from the work of the DIERS group. In these models it is assumed that vapour and liquid remain in thermal equilibrium during pressure relief and level swell is computed from an integral formulation based on the drift-flux model, i.e. an assumption is made about the distribution of vapour generation in the vessel and the drift-flux model is used locally to quantify momentum interactions between vapour and liquid. Even in multidimensional models (such as [2]) the assumption of thermal equilibrium implies an assumption about the distribution of vapour generation in the flashing two-phase mixture.

The results obtained from a one-dimensional equilibrium model are compared to experimental data in Fig. 1.

The equilibrium model clearly does not predict the initial steep pressure drop due to boiling delay and the strong rise of the liquid level during the first violent stage of flashing. During the initial transient the liquid level may reach values well above the equilibrium model predictions. These shortcomings are not surprising. First of all the assumption of thermal equilibrium is invalid shortly after the activation of the pressure relief system because a certain liquid superheat is required before boiling begins. Thermal equilibrium is reached only when enough interfacial area has become available for evaporation. Moreover, the equilibrium model implies that vapour is generated in the two-phase mixture precisely at the rate required to maintain equilibrium (locally). In reality an important part of the overall vapour generation occurs at the vessel walls. With vapour generation at the vessel wall, the void fraction distribution in the vessel (and therefore also the level swell) is different from the equilibrium model predictions, even during quasi-steady pressure relief after the initial transient. Therefore, thermal non-equilibrium affects both transient and quasi-steady level swell. The model presented in the following section incorporates non-equilibrium vapour generation and should correctly predict transient level swell.

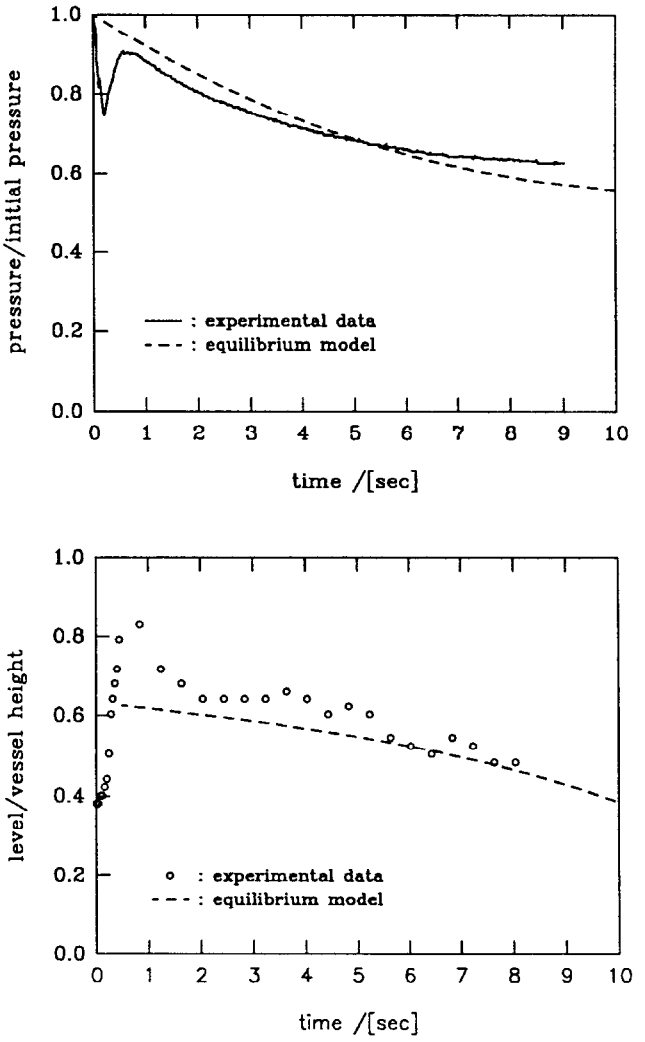

Fig. 1. Equilibrium model compared to experimental data.

3. Non-equilibrium model

3.1. Void propagation equations

In this section a non-equilibrium model is presented for transient level swell during depressurization of a top-vented vertical cylindrical vessel partially filled with a saturated liquid.

The description of void fraction propagation presented here, parallels an analytical model by Vea and Lahey [2]. Their model however is only valid if thermal equilibrium is assumed.

It is assumed that the two-phase flow in the bulk two-phase region is one-dimensional. Velocities in any direction but the mean flow direction are neglected. From the local-instantaneous continuity equations for two-phase flow [3], combined with the drift-flux model [4], the following equations are obtained

$$\frac{\partial}{\partial z} \ll j \gg = (v_v - v_l) \ll \Gamma \gg + \frac{\dot{v}_v}{v_v} \ll \varepsilon \gg, \tag{1}$$

$$\frac{\partial}{\partial t} \ll \varepsilon \gg + \left[C_0 \ll j \gg + \left(\frac{d\tilde{w}_{vj}}{d \ll \varepsilon \gg} \right) \ll \varepsilon \gg + \tilde{w}_{vj} \right] \frac{\partial}{\partial z} \ll \varepsilon \gg$$

$$= v_v \ll \Gamma \gg \left(1 - C_0 \left(1 - \frac{v_l}{v_v} \right) \ll \varepsilon \gg \right) + \frac{\dot{v}_v}{v_v} (1 - C_0 \ll \varepsilon \gg), \tag{2}$$

with

$$\tilde{w}_{vj} = C_1 \left(\frac{\sigma g \Delta \rho}{\rho_l^2} \right)^{0.25} (1 - \ll \varepsilon \gg)^n. \tag{3}$$

The first equation can be directly integrated and yields the total volumetric flux j of vapour and liquid. From the second equation it can be seen that void fraction changes due to evaporation and due to expansion of the vapour. The propagation of void fraction is governed by the drift-flux model coefficients C_0, C_1 and n.

3.2. Non-equilibrium vapour generation

The mass rate of vapour generation per unit of volume (Γ) is proportional to the interfacial area density and to the local mass flux through the interface (m''_{lv}), which is obtained from the energy jump equation

$$m''_{lv} = \frac{q''_{ll} + q''_{vl}}{\Delta h_{lv}}. \tag{4}$$

The heat fluxes q''_{kl} from the bulk phase k toward the interface are proportional to the difference between the bulk temperature T_k and the interface temperature, which is assumed to equal the saturation temperature. Then the following expression for Γ is obtained

$$\Gamma = \left(\frac{P_i}{A} \right) \frac{\alpha''_{ll} \cdot (T_l - T_{sat}(p)) + \alpha''_{vl} \cdot (T_v - T_{sat}(p))}{\Delta h_{lv}}. \tag{5}$$

Here P_i represents the total interfacial perimeter in cross-section A. The fraction P_i/A is referred to as the *interfacial area density*.

If the vapour phase is not moving relative to the liquid, then the rate coefficient α''_{ll} should be consistent with the growth law for a single growing bubble. Taking for

instance the Plesset–Zwick bubble growth law [5], the heat flux from the liquid to the bubble interface becomes

$$q''_{\mathrm{il}} = \rho_{\mathrm{v}} \Delta h_{\mathrm{lv}} \frac{dR}{dt} = \rho_{\mathrm{v}} \Delta h_{\mathrm{lv}} \frac{6\mathrm{Ja}^2 \kappa}{\pi R} \tag{6}$$

and therefore:

$$\alpha''_{\mathrm{il}} = \frac{6\pi}{R} k_{\mathrm{l}} \mathrm{Ja}. \tag{7}$$

This result was also obtained by Berne [6].

For a moving bubble, convection heat transfer can become more important than conductive heat transfer. For this case Ruckenstein [7] proved that

$$\mathrm{Nu}_R = \sqrt{\frac{2}{\pi} \mathrm{Pe}_R} \tag{8}$$

or

$$\alpha''_{\mathrm{il}} = \frac{k_{\mathrm{l}}}{R} \sqrt{\frac{2}{\pi} \frac{Rw_\infty}{\kappa_{\mathrm{l}}}}. \tag{9}$$

For the rate coefficient α''_{vl} no good models are presently available. Usually it is assumed that this coefficient is much larger than the rate coefficient at the liquid side. In this case a perfect thermal contact at the vapour side ($\alpha''_{\mathrm{vl}} = \infty$ or $T_{\mathrm{v}} = T_{\mathrm{sat}}(p)$) can be assumed without introducing significant errors.

At present little experimental information is available related to the interfacial area in two-phase flows. For the bubbly or churn-turbulent two-phase flow in a vertical vessel which occur during pressure relief, it is proposed here to compute the interfacial area density from

$$\frac{P_{\mathrm{i}}}{A} = \frac{3\varepsilon}{\bar{R}} (1 - \varepsilon)^{1/2} \tag{10}$$

with the average bubble radius $\bar{R}$ as an adjustable parameter. For low void fractions, this expression corresponds to a hypothetical situation of equally sized spherical bubbles. For high void fractions, the predicted interfacial area approaches zero, and the maximum interfacial area density is assumed to occur at the point of closest packing for spherical bubbles ($\varepsilon = 2/3$).

3.3. Boundary condition at the vessel wall

Any vapour which is generated at the vessel walls (including the bottom) should be taken into account as a source term (or a boundary condition for the vessel bottom). Vapour generation at the wall depends on non-equilibrium effects such as heterogen-

eous nucleation and conduction-controlled bubble growth. The authors have developed a model for vapour generation at vessel walls in a flashing liquid in [8]. This model combines a kinetic description of heterogeneous nucleation, an expression for thermally controlled bubble growth and a balance equation for the number of bubbles adhering to the wall, and yields an expression for the effective bubble generation rate $\dot{N}_{\mathrm{nuc}}$

$$\frac{1}{\dot{N}_{\mathrm{nuc}}} = \frac{1}{\dot{N}_{\mathrm{nuc,\,0}}} + \frac{1}{\dot{N}_{\mathrm{nuc,\,s}}} \tag{11}$$

with $\dot{N}_{\mathrm{nuc,0}}$ representing the kinetic limit to the nucleation rate (for instance according to [9]) and with

$$\frac{1}{\dot{N}_{\mathrm{nuc,\,s}}} = \frac{(\pi/2)^3}{3}\left(\frac{R_{\mathrm{d}}^4 - R_{\mathrm{c}}^4}{\mathrm{Ja}^2\,\kappa}\right). \tag{12}$$

At low superheat the effective bubble generation rate is dominated by the first term in (11), i.e. by the kinetic limit to the nucleation rate. At higher superheats however the solid surface becomes almost entirely filled with adhering bubbles. Then the effective bubble generation rate is governed by the bubble growth rate.

3.4. Energy balance equations

In the foregoing sections equations have been presented for vapour generation and vapour separation in the two-phase mixture. In order to obtain a complete pressure relief and level swell model, these equations have to be complemented with thermodynamic balance equations (for mass, internal energy and volume).

Contrary to the void propagation equations which are one-dimensional, the thermodynamic balance equations are written in a (zero-dimensional) volume-averaged form. This requires that pressure is uniform throughout the system and that macroscopic regions exist in which the temperature is sufficiently uniform. The volume averaged balance equations are written separately for the two-phase mixture and for the vapour dome. The derivation of these equations is discussed in [10].

4. Experimental verification

4.1. Experimental set-up and test conditions

Small-scale experiments were carried out to verify the pressure relief model and to quantify some of its parameters.

The experiments are carried out in a transparent 10 l test vessel (see Fig. 2). This vessel is connected to a large catch tank by a vertical vent line which contains a replaceable orifice plate and a fast action ball valve. Pressure relief is initiated by activating the ball valve.

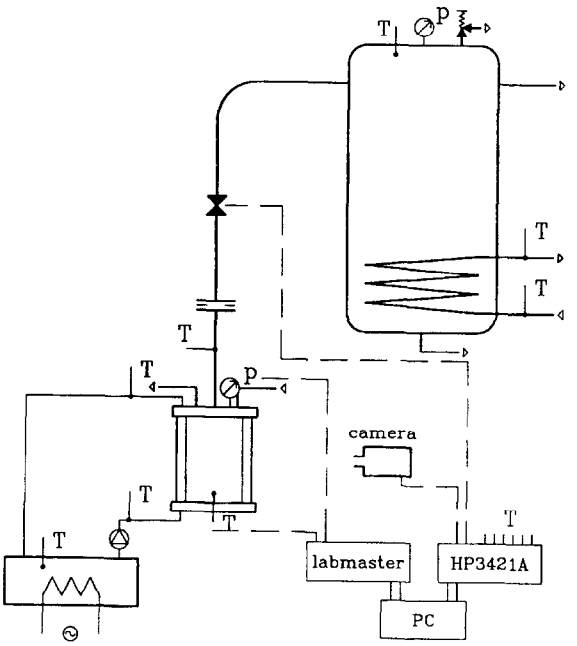

Fig. 2. Experimental set-up.

The vertical wall of the test vessel consists of two concentric Duran glass cylinders. Demineralized water is circulated through the space between the cylinders for heating or cooling the vessel contents. The ventline is a 50 mm diameter stainless steel tube, which is electrically heated to prohibit condensation in the ventline. At 0.5 m from the test vessel an orifice plate can be placed between two flanges. At 1 m from the test vessel a fast action (50 mm diameter) ball valve is located, which is pneumatically activated. The ventline connects to a 2 m^3 catch tank, which can be evacuated. A condenser is provided to recuperate the test fluid from the catch tank, and to guarantee that the catch tank pressure remains low during the execution of a test.

The experiments reported here are performed with R-113 as the working fluid. The initial temperature (before pressure relief) is always kept at 50 °C. The initial pressure in the test vessel is the corresponding vapour pressure (p = 1.092 bar). The superheat is varied by using different pressures in the catch tank. All experiments are performed with the same stainless steel bottom plate. The plate thickness is 10 mm; its surface is grounded and polished to a mirror finish.

The parameters that are varied during the experiments are as follows.

(1) The liquid superheat with respect to the catch tank pressure;
(2) The initial liquid level;
(3) The cross-section of the orifice plate in the vent line.

4.2. Comparison between model and experiments

In order to evaluate the performance of the pressure relief model, simulations have been carried out for the conditions of the small-scale experiments. For every parameter which is varied, the experimental data show a specific trend. In general all trends are well represented by the model. As an example, a comparison between model and experiments for different vent line orifice cross-sections is shown in Fig. 3. Similar comparisons have been performed for the other parameters [10].

The evaluation of the pressure relief model has indicated that the computed results depend on the following parameters:

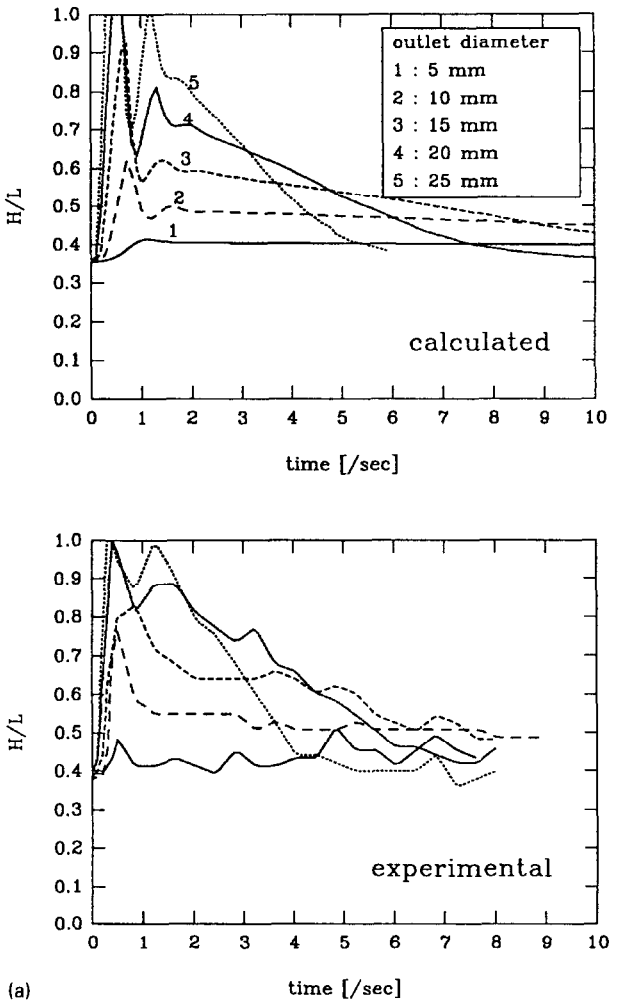

Fig. 3. Comparison between model and experiments for different ventline orifice cross-sections.

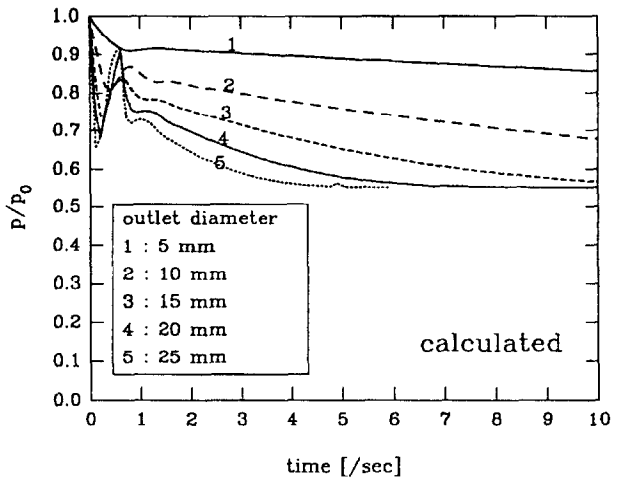

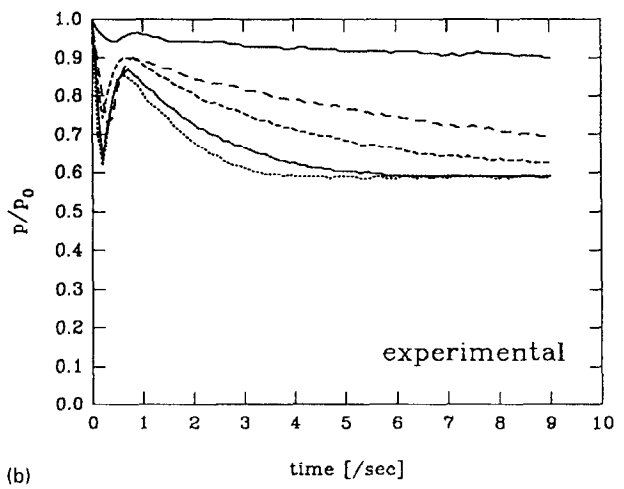

(b)

Fig. 3. Continued.

1. The distribution coefficient C_0 and the velocity coefficient C_1 of the drift-flux model;
2. The heterogeneity factor F of the vessel walls;
3. The average bubble radius $\bar{R}$ of the vapour bubbles in the two-phase mixture.

For the comparison between model and experiments shown in Fig. 1, the following values have been used:

$$C_0 = 1, \quad C_1 = 1.5, \quad F = 10^{-7}, \quad \bar{R} = 0.005 \text{ m}.$$

5. Evaluation of non-equilibrium effects

Based on results obtained from the new transient non-equilibrium pressure relief model, and on experimental results, the following general conclusions about the influence of thermal non-equilibrium have been obtained.

First of all a distinction must be made between transient and quasi-steady level swell. Non-equilibrium affects *both* transient and quasi-steady level swell, but in different ways.

During the initial transient the liquid level rises violently as the vapour which is generated in the surface layer and in the bulk mixture has not yet reached the liquid surface. The maximum value to which the level swell attains during the transient can be well above the quasi-steady level swell, and depends on the superheat attained during boiling delay, and on the interfacial area density in the bulk two-phase mixture. Quite evidently transient level swell should be considered when estimating the amount of fluid expelled from the vessel during pressure relief.

The relation between thermal non-equilibrium and transient level swell is not surprising. Thermal non-equilibrium does however also affect the value of the level swell once quasi-steady conditions have been reached. When thermal non-equilibrium is taken into account, the vertical distributions of void fraction and vapour generation are different from the corresponding distributions at equilibrium. The non-equilibrium distributions depend on the interfacial area density and on the vapour generation rate in the surface layer at the vessel bottom wall. As the latter depends on the wall temperature, the thermal response time of the wall also influences the quasi-steady value of the level swell.

Through parametric analysis the parameters which significantly affect level swell during pressure relief have been identified. They are as follows.

1. The distribution coefficient and the velocity coefficient of the drift-flux model describing the rate at which vapour separates from the two-phase mixture;
2. The interfacial area density which depends on the average bubble size in the two-phase mixture (quantified with the Sauter mean diameter);
3. The nucleation characteristics of the vessel bottom wall (quantified with the heterogeneity factor) and its thermal response time.

It should be mentioned that the important non-equilibrium behaviour exhibited by the experimental results (e.g. Fig. 2) are due to the small scale of these experiments. An analysis of scale effects for the transient level swell problem has been presented in [10]. Summarizing the results of this scale analysis it can be said that the magnitude of the boiling delay is inversely proportional to the linear system scale l, i.e.

$$\Delta T_{\max} \sim l^{-1}, \tag{13}$$

while the maximum level swell during the initial transient scales as

$$\frac{H_{\max}}{L} \sim 1 + Cl^{-1} \tag{14}$$

with a positive constant C. Therefore, non-equilibrium effects which are prominently present in small-scale experiments (or simulations), are far less pronounced in large-scale cases. This conclusion does however only apply to transient level swell. The effects of non-equilibrium on quasi-steady level swell are less obvious, and are independent of the system scale, as shown in [11].

6. Conclusion

A new one-dimensional non-equilibrium model for transient level swell during pressure relief has been developed and small-scale pressure relief experiments have been performed to evaluate the model. Both transient and quasi-steady level swell are affected by non-equilibrium vapour generation (at the vessel walls and in the bulk two-phase mixture). Due to scale effects the influence of thermal non-equilibrium is most pronounced for small size vessels.

Nomenclature

A	vessel cross-section area, m^2
C_0	distribution coefficient for drift-flux model
C_1	velocity coefficient for drift-flux model
F	heterogeneity factor for heterogeneous nucleation rate model
j	local volumetric flux, m/s
Ja	Jakob number
H_{max}	maximum height of two-phase mixture during pressure relief, m
k	thermal conductivity, W/mK
L	vessel length, m
l	linear system scale (e.g. $l = L$), m
m''_{lv}	local mass flux through vapour–liquid interface, $kg/(m^2\,s)$
$\dot{N}$	number of bubbles generated per unit surface and per unit time, $1/(m^2\,s)$
p	absolute pressure, N/m^2
P_i	cross-section area averaged interfacial perimeter, m
Pe	Peclet number
q''_{kI}	local heat transfer from bulk part of phase k to interface, W/m^2
R	bubble radius, m
$\bar{R}$	Sauter mean bubble radius, m
R_c	critical bubble radius, m
R_d	detachment bubble radius, m
t	time, s
T	temperature, K
v	specific volume, m^3/kg
$\dot{v}$	rate of change of specific volume, $m^3/(kg\,s)$

$\tilde{w}_{vj}$	phase-averaged drift velocity, m/s
z	vertical position, m

Greek symbols

α''_{kI}	local heat transfer coefficient between phase k and interface, W/(m^2 K)
Δh_{lv}	specific enthalpy difference between saturated vapour and liquid, J/kg K
$\Delta\rho$	specific volume difference between saturated vapour and liquid, kg/m^3
ΔT_{max}	maximum liquid superheat during pressure relief, K
ε	local void fraction
κ	thermal diffusivity, m^2/s
Γ	volumetric mass rate of vapour generation, kg/m^3 s
ρ	density, kg/m^3
σ	surface tension, N/m

Indices and averaging operator

l	liquid
v	vapour
sat	saturation
$\prec x \succ$	cross-section area averaged value of property x

References

[1] H.G. Fischer, H.S. Forrest, S.S. Grossel, J.E. Huff, A.R. Muller, J.A. Noronha, D.A. Show and B.J. Tilley, Emergency Relief System Design Using Diers Technology – The Design Institute for Emergency Relief Systems (DIERS) Project Manual, AIChE, New York, USA, 1992.
[2] H.W. Vea and R.T. Lahey Jr., Nucl. Engng. & Design, 45 (1978) 101–116.
[3] J.M. Delhaye, in: Durst (Ed.), Two-phase flow fundamentals, Two-phase momentum, heat and mass transfer in chemical, process and energy engineering systems, Int. Centre Heat & Mass Transfer, Belgrade, Yugoslavia, 1979.
[4] N. Zuber and J.A. Findlay, ASME J. Heat Transfer, 87 (1965) 453–468.
[5] M.S. Plesset and S.A. Zwick, J. Appl. Physics, 25 (1954) 493–500.
[6] P. Berne, Analyse critique des modeles de taux d'autovaporisation utilises dans le calcul des ecoulements diphasiques en conduite, Report CEA-R-5205, CEN Grenoble (F), 1983.
[7] E. Ruckenstein, Chem. Eng. Sci., 10 (1959) 22–30.
[8] B. Boesmans and J. Berghmans, in: Proc. 10th Internat. Heat Transfer Conf., Brighton, UK, 15-16/9, 1994.
[9] I. Thormahlen, in: Proc. 8th Int. Heat Transfer Conf., San Francisco, CA, USA, 1986.
[10] B. Boesmans, Transient level swell during emergency pressure relief of liquefied gases, Ph.D. Thesis, K.U. Leuven, Dept. of Mechanical Engineering, Leuven, Belgium, September 1994.
[11] B. Boesmans and J. Berghmans, J. Loss Prevention, 8 (1995) 3–10.